

## Electrogenerated chemiluminescence. 52. Binuclear iridium(I) complexes

Gary S. Rodman, and Allen J. Bard

*Inorg. Chem.*, **1990**, 29 (23), 4699-4702 • DOI: 10.1021/ic00348a023

Downloaded from <http://pubs.acs.org> on January 26, 2009

### More About This Article

---

The permalink <http://dx.doi.org/10.1021/ic00348a023> provides access to:

- Links to articles and content related to this article
- Copyright permission to reproduce figures and/or text from this article



estimates relying on metal-metal distance and size or  $\pi$  alternancy of the bridging ligand.<sup>5b</sup> The contributions from very different kinds of metal fragments to the  $\pi$  overlap with one specific ligand bridge are certainly more difficult to predict; however, intensities of pertinent charge-transfer transitions can serve as useful guidelines.<sup>25b</sup> This approach has triggered the successful search for organometallic  $d^5/d^6$  ( $\mu$ -pyrazine) analogues of the Creutz-Taube ion that display more intense charge-transfer transitions and much larger values of  $K_c$  than the inorganic parent system.<sup>25</sup> Considering these more practically oriented rules for electronic

coupling in addition to the well-known statistical and solvational contributions to  $K_c$ , it should thus be possible for experimentally working chemists to rationally design and synthesize new mixed-valence systems with very large stability constants.<sup>7,25</sup>

**Acknowledgment.** This work was generously supported by the Deutsche Forschungsgemeinschaft and Stiftung Volkswagenwerk. We also thank Degussa AG for donations of precious metal chemicals and Dr. Sylvia Ernst (Frankfurt) for preliminary experiments.

Contribution from the Department of Chemistry,  
The University of Texas at Austin, Austin, Texas 78712

## Electrogenerated Chemiluminescence. 52. Binuclear Iridium(I) Complexes

Gary S. Rodman and Allen J. Bard\*

Received November 14, 1989

The electrochemistry and electrogenerated chemiluminescence (ECL) of  $[\text{Ir}(\text{COD})(\mu\text{-L})_2]$ , where COD is 1,5-cyclooctadiene and L is the anion of pyrazole (pz) and substituted derivatives 3-methylpyrazole (mpz) and 3,5-dimethylpyrazole (dmpz), were studied in tetrahydrofuran (THF)/0.3 M tetra-*n*-butylammonium hexafluorophosphate (TBAH). A reversible 1-electron oxidation was observed for all compounds, with the potential of the wave shifting to more negative potentials with increasing substitution of the bridging ligands. An irreversible 1-electron reduction was observed for all three compounds, attributed to a following reaction of the reduction product. The electrode reaction appears more reversible with increasing substitution of the bridging ligands, and the rate constant of the reaction following reduction of the compounds was found to decrease from  $30 \pm 10 \text{ s}^{-1}$  for L = pz to  $0.33 \pm 0.09 \text{ s}^{-1}$  for L = dmpz. ECL was produced upon sequential generation of  $\text{Ir}_2^+$  and  $\text{Ir}_2^-$  by pulsing the potential of a Pt working electrode (at 20 Hz) between the anodic and the cathodic peak potentials. The emission is characteristic of the  $^3\text{B}_2$  excited state of  $\text{Ir}_2$  previously observed in the photoluminescence spectra of these compounds. ECL was also observed by oxidizing the  $\text{Ir}_2$  compounds in solutions containing TBA oxalate.

### Introduction

We report a study on the electrogenerated chemiluminescence (ECL) of  $[\text{Ir}(\text{COD})(\mu\text{-L})_2]$ , where COD is 1,5-cyclooctadiene and L is the anion of pyrazole (pz) and the substituted derivatives 3-methylpyrazole (mpz) and 3,5-dimethylpyrazole (dmpz). Much of the literature on the ECL of metal complexes is concerned with only a few types of coordination compounds such as  $\text{Ru}(\text{II})$ <sup>1,2</sup> and  $\text{Os}(\text{II})$ <sup>3,4</sup> tris chelates (bipyridine or phenanthroline) and molybdenum(II) halide clusters.<sup>5,6</sup> While many binuclear complexes containing two  $d^8$  transition metals have been found to luminesce strongly and to have accessible oxidized and reduced states, little work has been carried out on their ECL properties. Some studies of ECL from  $[\text{Pt}_2(\mu\text{-P}_2\text{O}_5\text{H}_2)_4]^{4-}$  have been reported by our group and others.<sup>7,8</sup> Studies of this complex were hampered by the instability of the difficult-to-characterize reduced species  $[\text{Pt}_2(\mu\text{-P}_2\text{O}_5\text{H}_2)_4]^{5-}$ . In this paper, we report the observation of ECL from solutions containing  $[\text{Ir}(\text{COD})(\mu\text{-L})_2]$  alone and in the presence of oxalate anion. These complexes have attracted much attention for their novel thermal<sup>9,10</sup> and photochemical<sup>11</sup> reactivities

and electrochemical<sup>12</sup> properties. The application of the ECL technique to this system should be useful in exploiting the electronic properties of the  $d^8$ - $d^8$  chromophore.

### Experimental Section

The compounds  $[\text{Ir}(\text{COD})(\mu\text{-pz})_2]$  (1),  $[\text{Ir}(\text{COD})(\mu\text{-mpz})_2]$  (2), and  $[\text{Ir}(\text{COD})(\mu\text{-dmpz})_2]$  (3), all abbreviated here as  $\text{Ir}_2$ , were prepared by the literature method.<sup>13</sup> Reagent grade tetrahydrofuran (THF) was predried over KOH and then twice distilled from sodium benzophenone ketyl. Tetrabutylammonium hexafluorophosphate (TBAH), used as the electrolyte, was recrystallized from EtOH followed by THF/ether. Tetrabutylammonium oxalate  $[(\text{TBA})_2\text{Ox}]$  was prepared by mixing tetrabutylammonium hydroxide and oxalic acid in a 2:1 molar ratio. The hygroscopic white solid was dried under high vacuum at room temperature for several days and stored in a drybox. The  $\text{Ir}_2$  and oxalate reagents were kept in separate storage bulbs on the cell and added to the electrolyte solution after collection of background data. The solvent was degassed by several freeze-pump-thaw cycles ( $<10^{-5}$  Torr) before being vacuum-transferred to a storage bulb on the electrochemical cell containing dry electrolyte. Alternatively, degassed THF was stored in a He-filled drybox and added to the cell in the drybox. A one-compartment cell was used for most experiments, except the coulometric measurements, in which a three-compartment cell was employed. The three-electrode configuration was used, with a Pt disk, flag, or gauze as the working electrode, Pt foil or gauze as the auxiliary electrode, and Ag wire as the reference electrode. The silver quasireference electrode (AgQRE)

- (1) Tokel, N. E.; Bard, A. J. *J. Am. Chem. Soc.* **1972**, *94*, 2862.
- (2) Gonzales-Velasco, J.; Rubinstein, I.; Crutchley, R. J.; Lever, A. B. P.; Bard, A. J. *Inorg. Chem.* **1983**, *22*, 822.
- (3) Abruña, H. D. *J. Electroanal. Chem. Interfacial Electrochem.* **1984**, *175*, 321.
- (4) Lee, C.-W.; Ouyang, J.; Bard, A. J. *J. Electroanal. Chem. Interfacial Electrochem.* **1988**, *244*, 319.
- (5) Ouyang, J.; Zietlow, T. C.; Hopkins, M. D.; Fan, F.-R. F.; Gray, H. B.; Bard, A. J. *J. Phys. Chem.* **1986**, *90*, 3841.
- (6) Mussell, R. D.; Nocera, D. G. *J. Am. Chem. Soc.* **1988**, *110*, 2764.
- (7) Vogler, A.; Kunkely, H. *Angew. Chem., Int. Ed. Engl.* **1984**, *23*, 316.
- (8) Kim, J.; Fan, F.-R. F.; Bard, A. J.; Che, C.-M.; Gray, H. B. *Chem. Phys. Lett.* **1985**, *121*, 543.

- (9) Coleman, A. W.; Eadie, D. T.; Stobart, S. R.; Zaworotko, M. J.; Atwood, J. L. *J. Am. Chem. Soc.* **1982**, *102*, 922.
- (10) Bushnell, G. W.; Fjeldsted, D. O. K.; Stobart, S. R.; Zaworotko, M. J. *J. Chem. Soc., Chem. Commun.* **1983**, 580.
- (11) Caspar, J. V.; Gray, H. B. *J. Am. Chem. Soc.* **1984**, *106*, 3029.
- (12) Boyd, D. C.; Rodman, G. S.; Mann, K. R. *J. Am. Chem. Soc.* **1986**, *108*, 1779.
- (13) Bushnell, G. W.; Fjeldsted, D. O. K.; Stobart, S. R.; Zaworotko, M. J.; Knox, S. A. R.; MacPherson, K. A. *Organometallics* **1985**, *4*, 1107.

**Table I.** Electrochemical and Corrected Photoluminescence Data for 1–3 in THF/0.3 M TBAH (CV Scan Rate = 200 mV/s; Potentials Referenced to the SCE)

compd	$E^{\circ}(\text{Ir}_2^{+/0})/\text{mV}$	$i_{\text{pc}}/i_{\text{pa}}$	$E^{\circ}(\text{Ir}_2^{0/-})/\text{mV}$	$i_{\text{pa}}/i_{\text{pc}}$	$\lambda_{\text{max}}(^3\text{B}_2)/\text{nm}$	$k_{\text{f}}^{\text{a}}/\text{s}^{-1}$
1	+0.342	1.0	-2.492	0.37	682	$30 \pm 10$
2	+0.318	1.0	-2.487	0.39		
3	+0.279	1.0	-2.510	0.65	714	$0.33 \pm 0.09$

<sup>a</sup>  $k_{\text{f}}$  = observed rate constant for the reaction following irreversible reduction of the  $\text{Ir}_2^-$  complexes.

was separated from the working electrode by a medium-porosity frit. The potential of the QRE was measured against the  $\text{Cp}^*_2\text{Fe}^{+/0}$  couple ( $\text{Cp}^*_2\text{Fe}$  = decamethylferrocene) in the sample solution at the end of the experiments. Measured potentials were referenced to the saturated calomel electrode (SCE), using a potential of -0.144 V vs SCE for the  $\text{Cp}^*_2\text{Fe}^{+/0}$  couple.<sup>14</sup> No  $iR$  compensation was used; rather, the importance of uncompensated resistance was assessed from the peak separation of the anodic and cathodic waves of the  $\text{Cp}^*_2\text{Fe}^{+/0}$  couple. Voltammetric and ECL experiments were performed with Princeton Applied Research Model 175 universal programmer, Model 173 potentiostat and Model 176 current follower. Chronocoulometry and bulk electrolyses were carried out with a Bioanalytical Systems BAS-100 electrochemical analyzer. The ECL spectra were obtained with a monochromator (Oriel Model 7240) with 0.2-mm slits and a single-photon-counting system (Hamamatsu Model C1230), which included a Hamamatsu R928 photomultiplier tube in a thermoelectronically cooled housing. The detector output was collected by a Norland Model 3001 digital oscilloscope and stored for subsequent plotting. These spectra were not corrected for detector response. Photoluminescence spectra were recorded on a Spex Fluorolog 2 spectrofluorometer and were corrected for detector response. Visible absorption spectra were obtained with a Hewlett-Packard Model 8450A diode-array spectrophotometer.

## Results and Discussion

**Electrochemistry of  $[\text{Ir}(\text{COD})(\mu\text{-L})_2]$ .** The cyclic voltammograms (CVs) of 1–3 ( $[\text{Ir}_2] = 2 \text{ mM}$ ) at 200 mV/s in THF containing 0.3 M TBAH are shown in Figure 1. The complexes display a quasireversible oxidation and a less reversible reduction. The formal potentials for the oxidative process, obtained by averaging the peak potentials ( $E_p$ ) of the anodic and corresponding cathodic reversal waves, are +0.342, +0.318, and +0.279 V vs SCE for 1–3, respectively, at 200 mV/s (Table I). The potential for the oxidative process is more negative with increasing methyl substitution of the bridging ligand, as expected for electron-donating alkyl substituents. The ratio  $i_{\text{pc}}/i_{\text{pa}}$  (where  $i_{\text{pa}}$  and  $i_{\text{pc}}$  are the peak currents for the anodic and cathodic (reversal) wave, respectively) at this scan rate was 1.0. The formal potentials for the reductive process are much less dependent on the bridging ligand substituents and are -2.492, -2.487, and -2.510 V for 1–3, respectively, at 200 mV/s vs SCE. At this scan rate, the ratio  $i_{\text{pa}}/i_{\text{pc}}$  was 0.37 for 1, 0.39 for 2, and 0.65 for 3. At faster scan rates,  $i_{\text{pa}}/i_{\text{pc}}$  for the reduction approaches 1.0 for all complexes. Thus, while the oxidized  $\text{Ir}_2$  species are stable on the CV time scale, the reduced species appear to undergo a following chemical reaction. The three small oxidation peaks that are seen on scan reversal following the cathodic peak between ca. -0.2 and -1.2 V vs SCE for each complex are ascribed to decomposition products formed upon reduction of the  $\text{Ir}_2$  compounds.

Previous studies<sup>12</sup> have demonstrated that the voltammetric response of 1 is highly sensitive to solvent and supporting electrolyte. For example, in acetonitrile, a single 2-electron quasireversible oxidation was observed. However, in very dry dichloromethane, the 2-electron wave was split into a quasireversible 1-electron wave and a second, irreversible 1-electron wave at a more positive potential. Several measurements carried out in this study with THF/TBAH established that under these conditions the oxidation in each compound is a 1-electron process. The peak separations  $E_{\text{pa}} - E_{\text{pc}}$  for 1–3 were 95 mV as was the peak separation of the reference  $\text{Cp}^*_2\text{Fe}^{+/0}$  couple. Since this latter couple follows Nernstian behavior in most solvents, the observed splitting greater than 58 mV suggests that uncompensated resistance affects the  $E_p$  values in all cases. Bulk coulometric oxidation of 3 at +0.454 V vs SCE resulted in the removal of  $1.0 \pm 0.1$  Faraday/mol ( $n_{\text{app}}$ ).

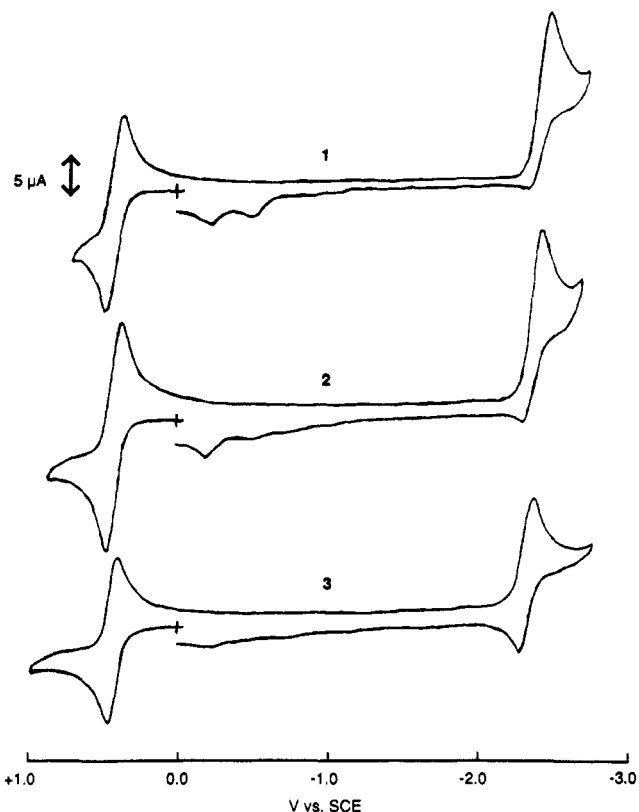


**Figure 1.** Cyclic voltammograms of 2 mM 1–3 in THF/0.3 M TBAH at a Pt electrode. Scan rate = 200 mV/s.

An absorption spectrum of the olive green oxidized solution showed bands at 440 and 496 nm as well as a very shallow, broad band at ca. 800 nm. These features are in excellent agreement with the spectrum of  $3^+$  observed in spectroelectrochemical studies carried out by Boyd and Mann.<sup>15</sup> The similar voltammetric behavior for 1 and 2 suggests that the oxidation observed for these compounds is also due to a 1-electron process. However, bulk electrolysis of 1 at +0.466 V resulted in  $n_{\text{app}} = 1.9 \pm 0.1$ . This result indicates that  $1^+$  undergoes a further reaction on the bulk electrolysis time scale ( $\sim 30$  min). It has been shown<sup>12</sup> that  $1^+$  reacts with halogenated solvents to give Ir(II)–Ir(II) products. A similar reaction to form either an Ir(II)–Ir(II) binuclear or an Ir(III) mononuclear species probably occurs in THF, although the exact product and mechanism are unknown at this time.

The observation that the peak current and peak separation of the reduction in each complex is comparable to that of the  $\text{Ir}_2^{+/0}$  couple suggests that the reductions are also 1-electron processes. However, the  $\text{Ir}_2^-$  species appear to undergo irreversible following chemical reactions. At 200 mV/s, three return oxidations are seen at -0.298, -0.583, and -0.958 V for 1, -0.282, -0.607, and -1.13 V for 2, and -0.330, -0.628, and -0.871 V for compound 3. For each complex, these oxidation waves are not observed when the reduction scan is reversed at potentials positive of the  $\text{Ir}_2^{0/-}$  couple, indicating that they are a consequence of generating  $\text{Ir}_2^-$ . The rate constant of the following reaction in 1 and 2 was estimated by measuring the peak current ratios  $i_{\text{pa}}/i_{\text{pc}}$  as a function of sweep rate. The data were analyzed by the method of Nicholson and Shain<sup>16</sup> for the case of an electron transfer followed by an irre-

(14) Under the conditions employed, the potential of the  $\text{Cp}^*_2\text{Fe}^{+/0}$  couple was 0.451 V more negative than that of  $\text{Cp}_2\text{Fe}^{+/0}$ .

(15) Boyd, D. C. Ph.D. Thesis, University of Minnesota, 1987.

**Table II.**  $i_{pa}/i_{pc}$  as a Function of Scan Rate for **1** and **3** with Estimated Rate Constants for the Reaction following Reduction of the  $\text{Ir}_2$  Complexes

compd 1			compd 3		
scan rate/ $\text{V}\cdot\text{s}^{-1}$	$i_{pa}/i_{pc}$	$k_f/\text{s}^{-1}$	scan rate/ $\text{V}\cdot\text{s}^{-1}$	$i_{pa}/i_{pc}$	$k_f/\text{s}^{-1}$
10	0.61	16	0.10	0.58	0.22
12	0.64	16	0.15	0.71	0.19
15	0.68	18	0.18	0.66	0.28
20	0.68	23	0.20	0.65	0.33
30	0.73	27	0.40	0.75	0.40
40	0.80	25	0.50	0.78	0.43
50	0.77	36	0.60	0.82	0.41
60	0.82	33	0.70	0.83	0.44
75	0.83	39	0.80	0.91	0.25
80	0.86	27	1.00	0.89	0.37
100	0.84	45			
125	0.88	42			0.33 ● 0.09 (av)
150	0.90	42			

30 ● 10 (av)

versible chemical reaction. A 25- $\mu\text{m}$  Pt microelectrode was required for measurements of **1** to achieve fast enough sweep rates to obtain significant reversal oxidation currents. The first-order rate constants ( $k_f$ ) for the disappearance of  $\text{Ir}_2^-$  are estimated to be  $30 \pm 10 \text{ s}^{-1}$  and  $0.33 \pm 0.09 \text{ s}^{-1}$  for **1** and **3**, respectively. Table II shows the data used to estimate the rate constants. It is clear that adding bulky substituents to the bridging ligand stabilizes the  $\text{Ir}_2^-$  moiety.

The relative insensitivity of the potentials of the  $\text{Ir}_2^{0/-}$  couple with respect to the bridging ligands suggests that the reduction is metal centered. Reductions of **1** or its analogues have not been previously reported, although formation of what are formally  $d^8$ - $d^9$  species is not unprecedented. Reductive quenching<sup>17</sup> of excited-state  $\text{Rh}_2(\mu\text{-L}_4)^{2+}$  and pulse radiolysis<sup>18</sup> of  $[\text{Rh}_2(\mu\text{-L}_4)]^{2+}$  and  $[\text{Pt}_2(\mu\text{-P}_2\text{O}_5\text{H}_2)_4]^{4-}$  have been found to produce short-lived 1-electron-reduced products. These reductions are thought to be metal centered. A 2-electron reduction of  $[\text{Pt}_2(\mu\text{-P}_2\text{O}_5\text{H}_2)_4]^{4-}$  by  $[\text{Cr}(\text{H}_2\text{O})_6]^{2+}$  has also been reported.<sup>19</sup> According to the qualitative molecular orbital scheme developed for  $d^8$ - $d^8$  complexes,<sup>20</sup> a metal-centered 1-electron reduction should add 1 electron to a low-lying  $p\sigma$  orbital (ground state  $^2A_2$  for  $C_{2v}$  symmetry), strengthening the M-M interaction as the formal bond order increases from zero to one-half. The observed instability of the  $\text{Ir}_2^-$  species may be due to the inability of the ligands to stabilize such electron-rich metal centers. Further experiments are required to characterize fully these  $\text{Ir}_2^-$  complexes.

**ECL of  $[\text{Ir}(\text{COD})(\mu\text{-L})_2$ .** ECL is produced upon alternate generation of  $\text{Ir}_2^+$  and  $\text{Ir}_2^-$  by pulsing the potential of a Pt working electrode (at 20 Hz) between the anodic peak potential of the oxidation and the cathodic peak potential of the reduction. The ECL of **1** and **3** was studied. The ECL spectra consist of a single band centered at 694 nm for **1** and 719 nm for **3**. These emission maxima correspond to the  $^3B_2$  emission<sup>21</sup> observed at 682 and 714 nm in the conventional photoluminescence spectra of **1** and **3** in THF/TBAH.<sup>22</sup> Shown in Figure 2 are the photoemission and

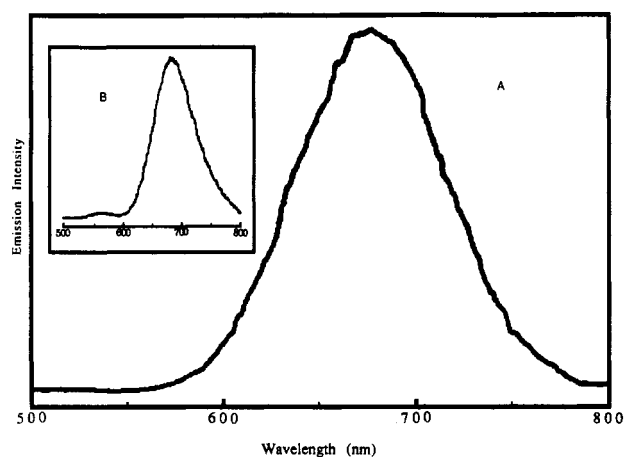
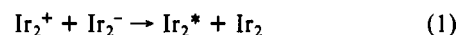


**Figure 2.** (A) Uncorrected ECL spectrum of 2.5 mM **1** in THF/0.3 M TBAH obtained by pulsing the potential of the working electrode between +0.35 and -2.50 V vs AgQRE at 20 Hz. (B) Corrected photoluminescence spectrum of **1** in THF/0.3 M TBAH,  $\lambda_{ex} = 480 \text{ nm}$ .

ECL spectra of **1**. The luminescent  $^3B_2$  species is formed by the annihilation reaction represented in eq 1. The driving force for



the electron-transfer reaction can be estimated from the CV data to be 2.9 and 2.8 eV for **1** and **3**, respectively. This is sufficient to populate both  $^1B_2$  and  $^3B_2$  states in the complexes ( $E_{0-0}$  values for  $^3B_2$  are estimated to be 2.06 and 1.97 V for **1** and **3**, respectively; the values for  $^1B_2$  are 2.46 and 2.37 V). The less intense  $^1B_2$  emission is not observed in the ECL spectra of either complex, probably because of self-absorption by the optically dense solutions employed in the electrochemical experiments.<sup>23</sup>

The ECL intensity of **3** is somewhat larger than that of **1**. Moreover, a passivating layer forms on the working electrode after prolonged pulsing between anodic and cathodic limits in the case of **1**. Both effects may be attributable to the more rapid decomposition of the  $\text{Ir}_2^-$  species of **1**. Some of the material produced in the reaction following the reduction probably precipitates on the working electrode.

ECL can also be produced by oxidizing  $\text{Ir}_2$  solutions that contain oxalate. In oxalate-containing systems, ECL is produced upon stepping the potential only in the region of anodic reactions, because a strongly reducing species ( $\text{CO}_2^-$ ) is produced during oxidation of oxalate.<sup>24</sup> This procedure circumvents problems with

- (16) Nicholson, R. S.; Shain, I. *Anal. Chem.* **1964**, *36*, 706. The first-order rate constant of the reaction following the reduction of  $\text{Ir}_2$  was estimated by measuring  $i_{pa}/i_{pc}$  at several scan rates and comparing them to the values of  $k_f\tau$  tabulated for case VI given in the reference. While in principle only one scan is necessary to estimate the rate constant, the reported rate constants are averaged for several scan rates (given in Table II). Only  $i_{pa}/i_{pc}$  values  $>0.5$  were used to minimize the uncertainty in measuring the return oxidation peak currents. The switching potentials used were -2.87 and -2.82 V for **1** and **3**, respectively.
- (17) Milder, S. J.; Goldbeck, R. J.; Kligler, D. S.; Gray, H. B. *J. Am. Chem. Soc.* **1980**, *102*, 6761.
- (18) Che, C.-M.; Atherton, S. J.; Butler, L. G.; Gray, H. B. *J. Am. Chem. Soc.* **1984**, *106*, 5143.
- (19) Alexander, K. A.; Stein, P.; Hedden, D. B.; Roundhill, D. M. *Polyhedron* **1983**, *2*, 1389.
- (20) Mann, K. R.; Gordon, J. G.; Gray, H. B. *J. Am. Chem. Soc.* **1975**, *97*, 3553.
- (21) Marshall, J. L.; Stobart, S. R.; Gray, H. B. *J. Am. Chem. Soc.* **1984**, *106*, 3027.
- (22) Small differences between the photoluminescence and ECL spectra are mainly due to the uncorrected detector response of the ECL apparatus.

- (23) Typically, the ECL spectra were obtained with  $[\text{Ir}_2] = 2.0\text{--}3.0 \text{ mM}$  and an optical pathlength of ca. 0.5 cm. The extinction coefficient of **1** at  $\lambda = 560 \text{ nm}$  ( $\lambda_{max}$  of the singlet emission) is approximately  $320 \text{ M}^{-1} \text{ cm}^{-1}$ , i.e., approximately 3.5% of the previously reported<sup>21</sup> extinction coefficient of  $9100 \text{ M}^{-1} \text{ cm}^{-1}$  for the  $\lambda_{max}$  of the singlet absorption. Thus, approximately 50-75% of any 560-nm ECL would be absorbed by the solution, making it difficult to observe the singlet emission under the experimental conditions employed. A similar situation exists for **3**.

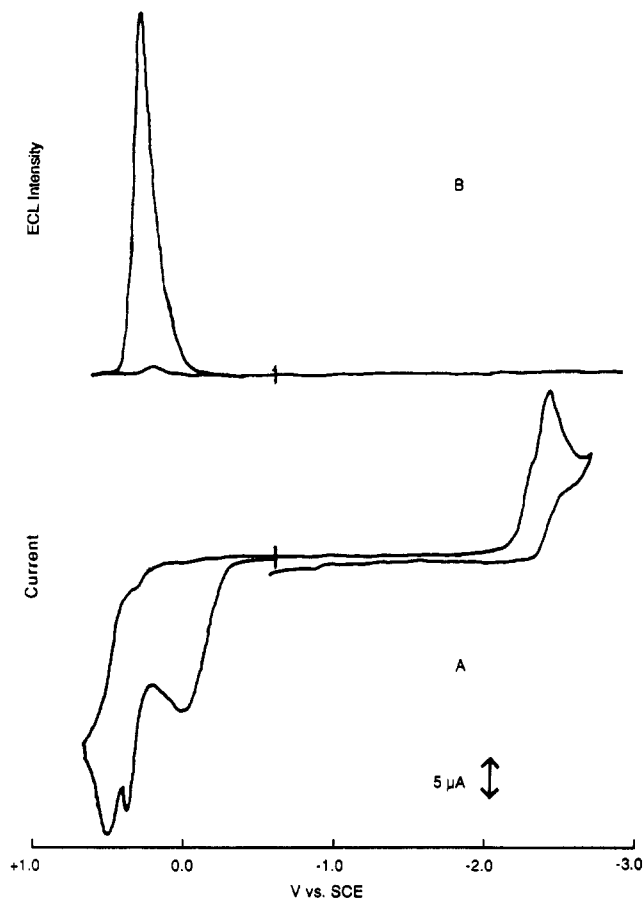
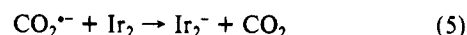
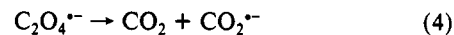
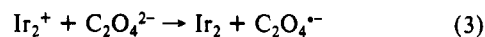


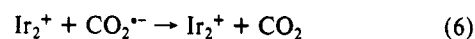
**Figure 3.** (A) Cyclic voltammogram of 2.5 mM **1** in the presence of a ca. 5-fold excess of  $(\text{TBA})_2\text{Ox}$  in THF/0.3 M TBAH. Scan rate = 200 mV/s. (B) ECL vs potential profile for solution in (A). The ECL spectrum was identical with that in Figure 2A.

the instability of the reduced reactant, e.g.,  $\text{Ir}_2^-$  in this study. The CV of a solution of **1** containing a 5-fold excess of  $(\text{TBA})_2\text{Ox}$  along with the ECL intensity vs potential profile is shown in Figure 3. The broad, irreversible oxidation at  $-0.77$  V (vs AgQRE) is due to oxidation of oxalate. ECL spectra of **1** and **3** in the presence of oxalate were obtained by pulsing the working electrode between  $+0.4$  and  $-0.1$  V at 50 Hz. The spectra produced by this method were essentially identical with those produced in the absence of oxalate by the  $\text{Ir}_2^{+/-}$  reaction (eq 1), although the ECL intensity was significantly larger when oxalate was used. The mechanism for producing ECL from single-potential-step oxidations of  $\text{Ir}_2$

solutions containing oxalate probably follows that proposed for the  $\text{Ru}(\text{bpy})_3^{2+}/\text{Ox}$  system.<sup>25</sup> The following scheme is proposed:



followed by (1) and/or



Note that, under the conditions employed here, oxalate is electrochemically oxidized at a potential less positive than that of the metal species and that the concentrations of  $\text{C}_2\text{O}_4^{2-}$ ,  $\text{C}_2\text{O}_4^{\bullet -}$ , and  $\text{CO}_2^{\bullet -}$  must be negligible at the electrode surface at potentials where  $\text{Ir}_2$  is oxidized. Thus, the reactions which lead to ECL, particularly reactions 3, 5, and 6, occur away from the surface, but probably within the diffusion layer.

The onset of ECL occurs just at the foot of the  $\text{Ir}_2$  oxidation wave, which grows in height, loses its cathodic reversal peak, and shifts to less positive potentials upon addition of oxalate. This behavior is characteristic of a catalytic ( $\text{EC}'$ ) reaction scheme, where the oxidized form reacts with a solution species to regenerate the parent species.<sup>25</sup> In this case a "prewave" on the  $\text{Ir}_2$  oxidation appears in the presence of oxalate, and the emission intensity maximizes at the potential of the prewave. A similar, but less pronounced, effect is found in the CV of **3** in the presence of oxalate. The ratio of the peak currents  $i_{pa}'/i_{pa}$  (where  $i_{pa}'$  is the peak current of the prewave) was independent of scan rate and increased with increasing oxalate concentration. The appearance of this prewave, which was reproducible, does not follow the usual considerations of an  $\text{EC}'$  reaction scheme, where the species that reacts with the electrogenerated oxidant is not directly oxidizable at the electrode in this potential region. Further studies are required to elucidate the detailed mechanism that gives rise to the observed electrochemical behavior of  $[\text{Ir}(\text{COD})(\mu\text{-L})_2]$  in the presence of oxalate.

In conclusion, we have shown that in THF solution, **1**–**3** can be oxidized and reduced in 1-electron reactions. Reduction affords the unstable species  $\text{Ir}_2^-$ , a formally  $d^8$ – $d^9$  species that is sufficiently long-lived to react with sequentially generated  $\text{Ir}_2^+$  to produce  $\text{Ir}_2^*$ . The excited-state species  $\text{Ir}_2^*$  can also be produced by simply oxidizing  $\text{Ir}_2$  in the presence of oxalate.

**Acknowledgment.** The support of this research by the National Science Foundation (Grant CHE8901450) is gratefully acknowledged.

(24) Ege, D.; Becker, W. C.; Bard, A. J. *Anal. Chem.* **1984**, *56*, 2413.

(25) Bard, A. J.; Faulkner, L. R. *Electrochemical Methods*; Wiley: New York, 1980; p 455.